

# Structural characterisation and spin glass behaviour of the new oxide $\text{Ba}_2\text{ScCoO}_5$

Inmaculada Julián Ortega,<sup>a</sup> Regino Sáez Puche,<sup>\*a</sup> Julio Romero de Paz<sup>b</sup> and José Luis Martínez<sup>c</sup>

<sup>a</sup>Departamento de Química Inorgánica, Facultad de CC. Químicas, Universidad Complutense de Madrid, Madrid-28040, Spain. E-mail: rsp92@eucmax.sim.ucm.es

<sup>b</sup>Facultad de CC. Experimentales y Técnicas, Universidad San Pablo CEU, Boadilla del Monte, Madrid-28660, Spain

<sup>c</sup>Instituto de Ciencia de Materiales CSIC, Cantoblanco, Madrid-28049, Spain

Received 10th July 1998, Accepted 10th November 1998

The new oxide  $\text{Ba}_2\text{ScCoO}_5$  has been synthesised by solid state reaction and characterised by using both X-ray and electron diffraction techniques. It crystallises in a perovskite-type structure, showing cubic symmetry, space group  $Pm\bar{3}m$  [ $a = 4.1400(9)$  Å].  $\chi_{dc}$  and  $\chi_{ac}$  magnetic susceptibility have been measured down to 1.6 K and analysed, indicating the existence of a freezing phenomenon corresponding to a spin glass state. In the high temperature range,  $\chi_{dc}$  shows a Curie–Weiss like behaviour, with magnetic correlations starting around  $T_C = 50$  K. Below this temperature, a strong irreversibility in  $\chi$  vs.  $T$  curves obtained by zero field cooled and field cooled processes (ZFC/FC) has been detected. A second magnetic transition to a spin-glass phase is observed at  $T_F = 35$  K in the ZFC curve.  $\chi_{ac}$  measurements performed at different frequencies and magnetic fields also show all the common features characteristic of re-entrant spin-glasses. A possible origin of this magnetic behaviour is proposed and discussed.

## Introduction

Previous studies concerning the family of compounds formed in the  $\text{BaO}–\text{Sc}_2\text{O}_3$  system have been carried out, showing that many of these materials are derived from the perovskite-type structure. The first member of this group is the oxide  $\text{Ba}_2\text{Sc}_2\text{O}_5$ , which has been described<sup>1</sup> as a distorted oxygen deficient perovskite exhibiting tetragonal symmetry ( $a = 4.517$  Å,  $c = 3.987$  Å).

More recently, several authors<sup>2–4</sup> have synthesised and performed some structural studies on the oxides resulting from partial substitution of scandium by copper. The structures are also perovskite based with  $\text{Ba}^{2+}$  occupying the twelve fold coordination A site, and Sc/Cu in the six fold coordination B site. These materials are oxygen deficient as a result of replacing  $\text{Sc}^{3+}$  by  $\text{Cu}^{2+}$ . The phases  $\text{Ba}_2\text{ScCuO}_{4+\delta}$  have been described as forming ‘double perovskite’ phases  $\text{A}_2\text{BB}'\text{O}_{6-x}$ , crystallising with tetragonal symmetry, space group  $P4/mmm$ . In these compounds, one Sc (B) has been fully substituted by one Cu (B') and both cations are ordered on two crystallographically different sites alternated along the  $c$ -axis, causing the doubling of the unit cell in this direction. The anionic vacancies are mostly localised in the Cu–O layers. In this work we have studied the effect of substituting cobalt cations for scandium in  $\text{Ba}_2\text{Sc}_2\text{O}_5$ , resulting in an oxide of composition  $\text{Ba}_2\text{ScCoO}_5$ .

The complex magnetic properties of cobalt compounds are well known. In this sense, the perovskite  $\text{LaCoO}_3$  constitutes a system which has been the object of many studies in recent years, due to the unusual variation of its magnetic and electric properties with temperature.<sup>5,6</sup> Goodenough and Señaris<sup>7</sup> describe a gradual evolution of the system: at low temperatures, almost all the cobalt exists as low spin  $\text{Co}^{3+}$  in octahedral coordination, although small concentrations of high spin  $\text{Co}^{3+}$  in a lower coordination can be detected at the surface or associated with lattice defects. When the temperature is increased, the proportion of high spin  $\text{Co}^{3+}$  increases, until a maximum ratio of high- to low-spin  $\text{Co}^{3+}$  of 50:50 is reached. The dynamic ordering between Co cations in both spin states stabilises this situation. The electric properties of the compound evolves from a semiconducting to a metallic behaviour

as a result of the changes in the spin state when the temperature is increased.

When doping with  $\text{Sr}^{2+}$  ( $\text{La}_{1-x}\text{Sr}_x\text{CoO}_3$ ), the substitution of  $\text{Sr}^{2+}$  for  $\text{La}^{3+}$  in the A positions of the perovskite introduces holes and leads to the appearance of  $\text{Co}^{\text{IV}}$  ( $t_2^5e^0$ ), which forms  $\text{Co}^{\text{IV}}\cdot 6\text{Co}^{3+}$  clusters in the structure.<sup>7</sup> Inside these clusters, ferromagnetic superexchange interactions  $\text{Co}^{3+}–\text{O}–\text{Co}^{\text{IV}}$  occur, while the interactions between different clusters are antiferromagnetic via  $\text{Co}^{3+}–\text{O}–\text{Co}^{3+}$  paths. The random distribution of  $\text{Sr}^{2+}$  in the lattice, and so of the cobalt clusters, and the mixture of different types of magnetic interactions, leads to a frustrated situation that is revealed as the typical spin glass behaviour exhibited by these materials.

There are other examples of cobalt oxides showing spin glass behaviour as for example, the system  $\text{BaCo}_6\text{Ti}_6\text{O}_{19}$ , which crystallises with the barium hexaferrite M-type structure. The magnetic frustration arises from the  $\text{Co}^{2+}$  random diluted distribution amongst the non-magnetic  $\text{Ti}^{4+}$  both cations occupying simultaneously the five metallic sublattices of the M-type structure.<sup>8</sup>

This work concerns the synthesis and structural determination of the oxide  $\text{Ba}_2\text{ScCoO}_5$ . A detailed study of the  $\chi_{dc}$  and  $\chi_{ac}$  behaviour has been performed in order to explain the unusual magnetic properties of this new compound.

## Experimental

$\text{Ba}_2\text{ScCoO}_5$  was prepared by a ceramic method, from stoichiometric amounts of  $\text{Sc}_2\text{O}_3$  (99.9%),  $\text{CoCO}_3 \cdot n\text{H}_2\text{O}$  (47% Co) and  $\text{BaO}_2$  (95%). The mixture was homogenised in an agate mortar and heated in air at 1040 °C for 24 h, to yield the oxide as a polycrystalline material.

For structural characterisation, two different techniques have been used. First, powder X-ray diffraction at room temperature was carried out on a Philips PW-1800 diffractometer using  $\text{Cu-K}\alpha$  radiation, in the angular range  $10 < 2\theta < 120^\circ$ , with step width  $0.04^\circ$  and a counting time of 12 s for each step. The diffraction patterns were analysed by the Rietveld method<sup>9</sup> using the FULLPROF program,<sup>10</sup> the profile function used for describing the peak shape was of

pseudo-Voigt type, and preferred orientations were not taken into account. Secondly, selected area electron diffraction studies were carried out in a JEOL 2000 FX II microscope and a Philips CM 200 FEG, both working at 200 keV.

$\chi_{dc}$  and  $\chi_{ac}$  magnetic susceptibility measurements were performed using a Quantum Design SQUID magnetometer MPMS-XL in the range 2–300 K.  $\chi_{ac}$  measurements were performed as a function of both frequency ( $1 < \omega < 1000$  Hz) and external magnetic field ( $50 < H < 1000$  Oe).  $\chi_{dc}$  susceptibility was measured using field cooled (FC) and zero field cooled (ZFC) processes at 100 Oe. The SQUID was calibrated using metallic Pd as standard, and the magnetic susceptibility data were corrected considering ionic diamagnetic contributions.

## Results and discussion

### Structural characterisation

The compound  $\text{Ba}_2\text{ScCoO}_5$  has been characterised by powder X-ray diffraction and SAED techniques. Fig. 1 shows the X-ray diffraction pattern observed and calculated using the Rietveld method for this oxide, as well as the difference between them. The refinements have been performed considering the aristotype perovskite as a model, in cubic space group  $Pm\bar{3}m$ , with cell parameter  $a = 4.1400(9)$  Å. The extra peaks observed at  $2\theta \approx 24, 31$  and  $52^\circ$ , correspond to small amounts of the hexagonal perovskite  $\text{BaCoO}_{3-x}$ , as confirmed by SAED. This impurity has not been considered in the Rietveld refinement because of the uncertainty in the value of  $x$ .

SAED patterns obtained along two different zone axes for  $\text{Ba}_2\text{ScCoO}_5$  are shown in Fig. 2. They confirm the proposed symmetry since they have been indexed taking the cubic cell obtained by X-ray diffraction refinements as a basis. This is indicative of a disordered occupation of the B sites of the perovskite by scandium (B) or cobalt (B') cations, as well as a random distribution of oxygen vacancies in the structure. The introduction of cobalt cations in the oxide  $\text{Ba}_2\text{Sc}_2\text{O}_5$ , eliminates the small distortion which makes this latter compound tetragonal, and the resulting  $\text{Ba}_2\text{ScCoO}_5$  oxide shows cubic symmetry. Comparing this situation with that previously described<sup>3</sup> for the system  $\text{Ba}_2\text{ScCuO}_{4+\delta}$ , where scandium and copper cations are ordered and the oxygen vacancies are mainly concentrated in the Cu–O planes resulting in a tetragonal superstructure (space group  $P4/mmm$ ), it can be inferred that the nature of B' ions has a great influence on the structure. To understand this difference we must take into account the different electronic configuration of cobalt and copper ions, which determines the number and nature of metal–oxygen bonds. Copper is known as a very versatile cation which readily adopts different coordinations, even in a fixed oxidation

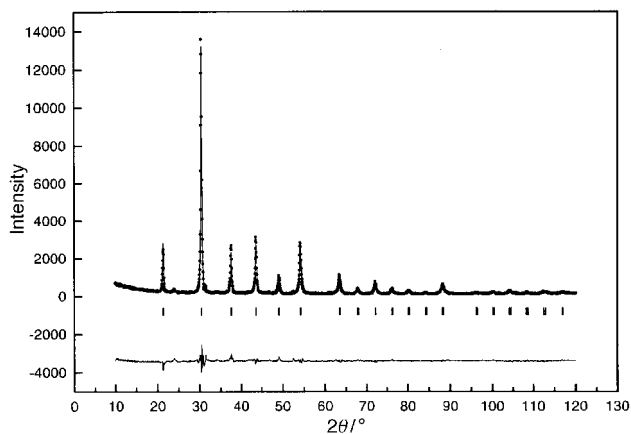


**Fig. 1** Observed (dots) and calculated (solid line) profiles for  $\text{Ba}_2\text{ScCoO}_5$ . The difference is plotted at the bottom. Reliability factors:  $R_{wp}$ : 20.9%,  $R_B$ : 7.09%,  $\chi^2$ : 4.37.

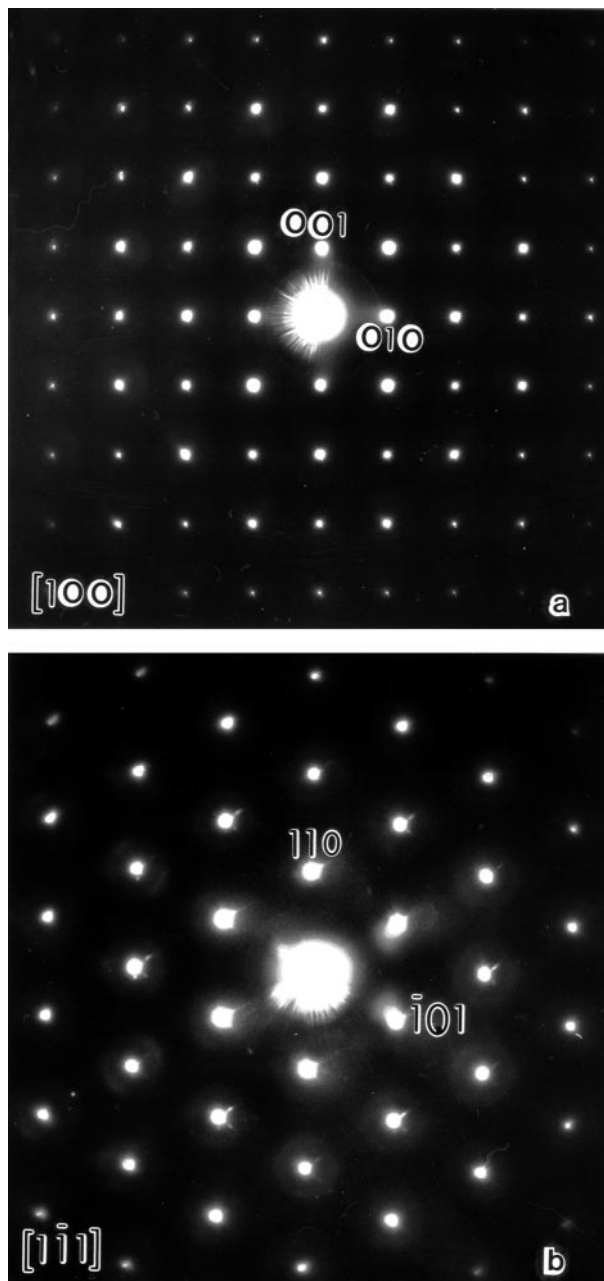


**Fig. 2** SAED patterns for the oxide  $\text{Ba}_2\text{ScCoO}_5$  obtained along the zone axes a)  $[100]$  and b)  $[1\bar{1}1]$ .

state.<sup>11</sup> In  $\text{Ba}_2\text{ScCuO}_{4+\delta}$ , copper is able to adapt itself to the coordinative changes derived from the formation of the superstructure, while cobalt shows the same preference for octahedral coordination as does scandium and, in this case, the disordered situation is more favourable.

Diffuse intensity surfaces around the diffraction maxima, which are especially marked along the  $[1\bar{1}1]$  zone axis [Fig. 2(b)] are associated with the existence of short range ordering of oxygen vacancies and/or scandium and cobalt cations along this direction. Nevertheless, they are local effects that do not affect the average cubic symmetry of the compound.

### Magnetic properties

Concerning the magnetic properties of  $\text{Ba}_2\text{ScCoO}_5$ , Fig. 3 shows the variation of the magnetic susceptibility with the temperature for this compound, cooling in the presence (FC) and absence (ZFC) of a magnetic field. Above 50 K, ZFC and FC susceptibilities are coincident. Fitting the data in the

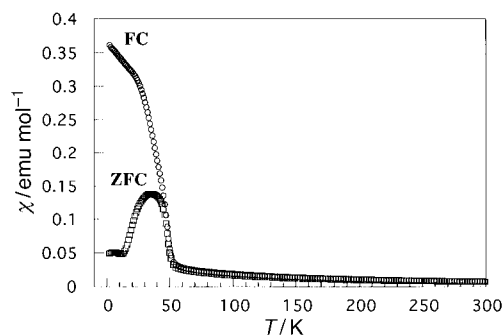


**Fig. 3** Temperature dependence of the magnetic susceptibility for  $\text{Ba}_2\text{ScCoO}_5$  cooling in the presence (FC, 100 Oe) and absence (ZFC) of an external magnetic field.

temperature range 300–50 K to a Curie–Weiss law, resulted in the parameters  $\theta = -48.78$  K and  $C = 1.96$  emu K mol<sup>-1</sup>. The calculated magnetic moment,  $3.96 \mu_B$ , is indicative of the coexistence of  $\text{Co}^{3+}$  in low and high spin states in this material. It should be noted that  $\text{Co}^{3+}$ , with electronic configuration  $3d^6$ , in octahedral coordination can adopt either high spin  $\text{Co}^{3+}$  ( $t_{2g}^4 e_g^2$ ) or low spin  $\text{Co}^{3+}$  ( $t_{2g}^6 e_g^0$ ) configurations. The energy gap has been reported to be as low as 0.08 eV, making the transition from the lower energy low spin state ( $^1A_1$ ) to the high spin state ( $^5T_2$ ) relatively facile.<sup>5</sup> In the case of  $\text{Ba}_2\text{ScCoO}_5$ , the estimated low spin  $\text{Co}^{3+}$  concentration is 36% of the total. At  $T = 50$  K the magnetic susceptibility sharply increases and below this temperature, ZFC and FC curves diverge, the ZFC susceptibility showing a broad maximum at 35 K and a small maximum at 7 K, decreasing to values as low as  $0.05$  emu mol<sup>-1</sup> at 2 K. The effect observed at 7 K can be attributed to the onset of antiferromagnetic interactions in the  $\text{Co}^{3+}$  sublattice, that becomes apparent at such low temperatures due to the random diluted distribution of the  $\text{Co}^{3+}$  magnetic cations in the B positions of the structure, amongst diamagnetic low-spin  $\text{Co}^{3+}$  and  $\text{Sc}^{3+}$  which break the superexchange paths. The variation of the product  $\chi T$  with temperature shown in Fig. 4 is very informative. It is observed that  $\chi T$  remains almost constant in the temperature range corresponding to the paramagnetic behaviour of the oxide (50–300 K). When the temperature is decreased below 50 K, a sharp increase of  $\chi T$  is detected, reaching a maximum value at 41 K and decreasing to zero at 2 K. The inflection observed at 7 K confirms the antiferromagnetic fluctuations previously mentioned.

Following the evolution of the system, we can distinguish two critical temperatures: first,  $T_C = 50$  K, when the magnetic susceptibility increases due to the onset of local ferromagnetic correlations between  $\text{Co}^{3+}$  cations, which leads to the formation of superparamagnetic clusters in the material. Below  $T_C$ , the FC curve lies above the ZFC one as a result of increased alignment of these ferromagnetic entities on cooling in the presence of a magnetic field. At low temperatures, as described

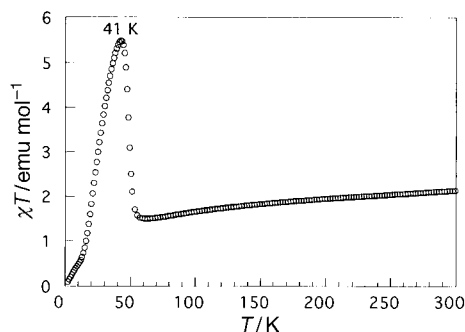


**Fig. 4** Variation with temperature of the product  $\chi T$  for the oxide  $\text{Ba}_2\text{ScCoO}_5$ .

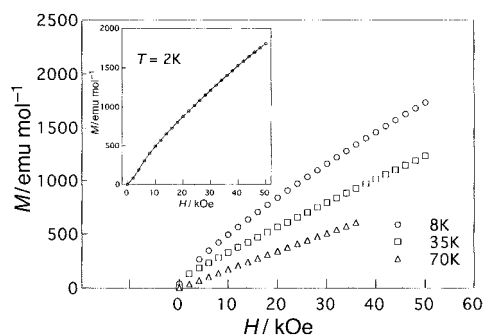


**Fig. 5** Magnetisation curves obtained at different temperatures for the oxide  $\text{Ba}_2\text{ScCoO}_5$ . The inset shows the magnetisation curve at 2 K (solid line is drawn to guide the eye).

in the literature for re-entrant spin glasses, the ferromagnetic component saturates. Second,  $T_G = 35$  K, the temperature corresponding to the magnetic susceptibility maximum in the ZFC curve, is attributed to blocking of interactions between the superparamagnetic clusters and associated with the freezing of the magnetic moments characteristic of spin-glass systems.

Magnetisation measurements provide useful information about the magnetic behaviour of this oxide below  $T_G$ . As it can be observed in Fig. 5, a straight line is only obtained above 70 K, when the material is paramagnetic. Curves below 70 K show a clear ferromagnetic component, with increasing importance as the temperature is lowered, which does not saturate even in fields as high as 50 kOe. At 2 K (Fig. 5, inset), a characteristic S-shape curve is obtained.

In order to gain a deeper insight in the spin-glass behaviour of this oxide, we have performed  $\chi_{ac}$  measurements as a function of temperature at different frequencies (Fig. 6) and magnetic fields (Fig. 7). In Fig. 6 it is shown that the real part of  $\chi_{ac}$  exhibits a maximum at 45 K which is slightly displaced towards higher temperatures and decreases in intensity as the frequency of the measurement is increased from 1 to 800 Hz, as described in the literature for canonical spin glasses.<sup>12</sup> Fig. 7

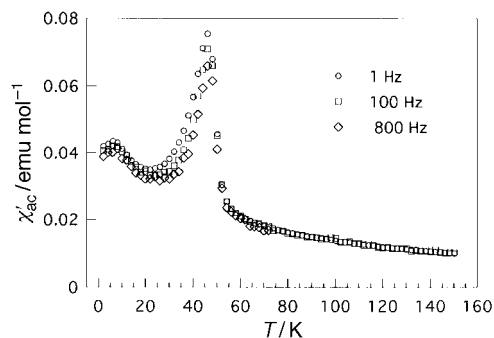


**Fig. 6** Temperature dependence of the real part of ac magnetic susceptibility measured at different frequencies.

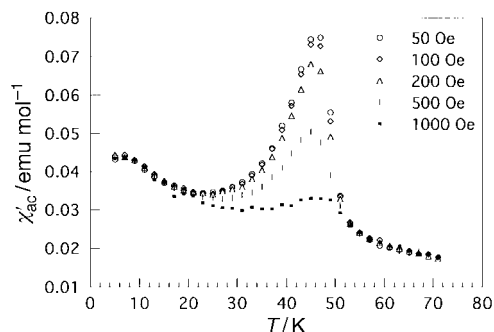


**Fig. 7** Temperature dependence of the real part of ac magnetic susceptibility measured with different external applied magnetic fields.

shows the strong influence of the magnetic field on the ac susceptibility: the maximum at 45 K gets flattened when increasing the field; this effect has also been observed in different spin glass systems such as NENP spin-glasses.<sup>13</sup>

All the measurements discussed in detail above, confirm the spin glass behaviour of the oxide Ba<sub>2</sub>ScCoO<sub>5</sub>. The origin of this spin glass behaviour could be first, due to chemical site disorder, which should contribute to the frustrated magnetic ground state. Secondly, competing ferromagnetic and antiferromagnetic interactions between nearest neighbours and next nearest neighbours in a cubic arrangement leads to an intrinsically frustrated magnetic ground state. A similar case has been recently reported for the spin glass compounds A<sub>2</sub>Mn<sub>2</sub>O<sub>7</sub> (A=rare earth), which show a cubic pyrochlore structure, where the ground state is a completely disordered system.<sup>14–15</sup> A wider investigation concerning the nature of the magnetic transitions that take place in Ba<sub>2</sub>ScCoO<sub>5</sub> at low temperatures by means of neutron diffraction studies is at present under way. The synthesis and study of different members of the family Ba<sub>2</sub>Sc<sub>2-x</sub>Co<sub>x</sub>O<sub>5</sub> (0.25 < x < 0.75) will also shed some light on the influence of the cobalt content on the magnetic properties of these oxides.

### Acknowledgements

We thank CICyT (Project MAT97–0697) for financial support. We are also indebted to Rhône-Poulenc for providing scandium oxide.

### References

- 1 W. Kwestroo, H. A. M. van Hal and C. Langereis, *Mater. Res. Bull.*, 1974, **9**, 1623.
- 2 A. L. Kharlanov, N. R. Khasanova, M. V. Paromova, E. V. Antipov, L. N. Lykova and L. M. Kovba, *Russ. J. Inorg. Chem.*, 1990, **35**, 1741.
- 3 D. H. Gregory and M. T. Weller, *J. Solid State Chem.*, 1993, **107**, 134.
- 4 D. H. Gregory and M. T. Weller, *J. Mater. Chem.*, 1994, **416**, 921.
- 5 P. M. Raccah and J. B. Goodenough, *Phys. Rev.*, 1967, **155**, 932.
- 6 P. Ganguly and C. N. R. Rao, *Bull. Mater. Sci.*, 1980, **2**, 193.
- 7 M. A. Señaris-Rodríguez and J. B. Goodenough, *J. Solid State Chem.*, 1995, **118**, 323.
- 8 X. Batlle, A. Labarta, B. Martínez, X. Obradors, V. Cabañas and M. Vallet, *J. Appl. Phys.*, 1991, **70**, 6172.
- 9 R. A. Young, *The Rietveld Method*, Oxford Science Pub., Oxford, 1995.
- 10 J. Rodríguez Carvajal, in *Abstracts Satellite Meet. Powder Diffraction 15th Congr. Int. Union Crystallography*, Toulouse, 1990, p. 127.
- 11 H. K. Müller-Buschbaum, *Angew. Chem., Int. Ed. Engl.*, 1991, **30**, 723.
- 12 J. A. Mydosh, *Spin Glasses: An Experimental Introduction*, Taylor and Francis, London, 1993.
- 13 M. Hagiwara, K. Katsumata, S. Sasaki, N. Narita, I. Yamada and T. Yosida, *J. Appl. Phys.*, 1996, **79**, 6167.
- 14 M. A. Subramanian, J. K. Greedan, N. P. Raju, A. P. Ramírez and A. M. Sleight, *J. Phys. IV*, 1997, **C1**, 625.
- 15 Y. Shimakawa, Y. Kubo, T. Manako, Y. V. Sushko, D. N. Argyriou and J. D. Jorgensen, *Phys. Rev. B*, 1997, **55**, 6399.

Paper 8/05389H